Atmospheric Environment 127 (2016) 347–354

Contents lists available at ScienceDirect

Atmospheric Environment

journal homepage: www.elsevier.com/locate/atmosenv

Light absorption by biomass burning source emissions

Yuan Cheng [a], Guenter Engling [b, *], Hans Moosmüller [b], W. Patrick Arnott [b, c], Antony L.W. Chen [b, d], Cyle E. Wold [e], Wei Min Hao [e], Ke-bin He [a, f, g]

[a] State Key Joint Laboratory of Environment Simulation and Pollution Control, School of Environment, Tsinghua University, Beijing, China
[b] Division of Atmospheric Sciences, Desert Research Institute, Reno, NV, USA
[c] Department of Physics, University of Nevada, Reno, NV, USA
[d] Department of Environmental and Occupational Health, University of Nevada, Las Vegas, NV, USA
[e] Fire Science Laboratory, USDA Forest Service, Missoula, MT, USA
[f] State Environmental Protection Key Laboratory of Sources and Control of Air Pollution Complex, Beijing, China
[g] Collaborative Innovation Center for Regional Environmental Quality, Beijing, China

HIGHLIGHTS

- Two distinct types of biomass smoke were identified by the MAE vs. OC/EC dependence.
- They also differed with respect to artifacts in the filter-based b_{abs} measurement.
- Present assessments of biomass burning BC emissions might be largely overestimated.
- Biomass burning emissions with high OC/EC ratios may include some liquid-like OM.
- These liquid-like organic components can complicate filter-based b_{abs} measurements.

ARTICLE INFO

Article history:
Received 21 July 2015
Received in revised form
1 December 2015
Accepted 17 December 2015
Available online 20 December 2015

Keywords:
Biomass burning
Light absorption
Black carbon
Photoacoustic
Liquid-like organics

ABSTRACT

Black carbon (BC) aerosol has relatively short atmospheric lifetimes yet plays a unique and important role in the Earth's climate system, making it an important short-term climate mitigation target. Globally, biomass burning is the largest source of BC emissions into the atmosphere. This study investigated the mass absorption efficiency (MAE) of biomass burning BC generated by controlled combustion of various wildland fuels during the Fire Laboratory at Missoula Experiments (FLAME). MAE values derived from a photoacoustic spectrometer (~7.8 m^2/g at a wavelength of 532 nm) were in good agreement with those suggested for uncoated BC when the emission ratios of organic carbon (OC) to elemental carbon (EC) were extremely low (i.e., below 0.3). With the increase of OC/EC, two distinct types of biomass smoke were identified. For the first type, MAE exhibited a positive dependence on OC/EC, while the overestimation of the light absorption coefficient (b_{abs}) by a filter-based method was less significant and could be estimated by a nearly constant correction factor. For the second type, MAE was biased low and correlated negatively with OC/EC, while the overestimation of b_{abs} by the filter-based method was much more significant and showed an apparent OC/EC dependence. This study suggests that BC emission factors determined by the commonly used thermal-optical methods might be sustantially overestimated for some types of biomass burning emissions. Our results also indicate that biomass burning emissions may include some liquid-like organics that can significantly bias filter-based b_{abs} measurements.

1. Introduction

Black carbon (BC) aerosol plays a unique and important role in the Earth's climate system through absorbing solar radiation, influencing cloud processes, and altering the melting behavior of snow and ice cover (Bond et al., 2013; Lack et al., 2014). As an important short-term climate mitigation target, however, BC has not been unambiguously defined yet due to the multitude of measurement principles. Consequently, reported BC data are dependent on the respective measurement techniques (Andreae

* Corresponding author.
E-mail addresses: ycheng@mail.tsinghua.edu.cn (Y. Cheng), Guenter.Engling@dri.edu (G. Engling).

http://dx.doi.org/10.1016/j.atmosenv.2015.12.045
1352-2310/

and Gelencsér, 2006; Baumgardner et al., 2012; Bond et al., 2013; Petzold et al., 2013; Buseck et al., 2014). In this paper, we adopt the terminology recommended by Petzold et al. (2013) and use the term BC to generally describe the carbonaceous materials in particles that are strongly light-absorbing in the spectral range of visible light, refractory, and insoluble.

Presently, global atmospheric absorption attributable to BC remains highly uncertain. The mass absorption efficiency (MAE; also known as the mass absorption cross section, MAC) is an essential factor converting BC mass concentration (in $\mu g/m^3$) simulated by chemical transport models to the absorption coefficient in the atmosphere (in m^{-1}) required for use in radiative transfer models. MAE of BC cannot be directly measured; instead, it is calculated as the absorption coefficient per BC mass (in this case, the determination of BC mass should be independent of optical absorption measurements).

Historically, the BC mass fraction of carbonaceous aerosol is most frequently quantified by filter-based methods such as thermal-optical measurements. BC mass determined by thermal-optical methods is commonly referred to as elemental carbon (EC). In thermal-optical analysis, EC can survive up to ~900 K in the presence of oxygen, and meanwhile, the removal (e.g., combustion) of EC leads to a rapid increase of the filter transmittance and reflectance which are typically monitored at 632 or 678 nm (Chow et al., 2004; Cavalli et al., 2010). Thus, EC is distinguished from other carbonaceous components (i.e., organic carbon) by its much higher thermal stability and considerably stronger light-absorbing capacity in the spectral range of red light. More recently, there have been growing applications of in-situ techniques to the determination of BC mass. Examples of these in-situ techniques include (1) aerosol mass spectrometric methods (e.g., the Aerosol Time-of-Flight Mass Spectrometer, ATOFMS, Pratt and Prather, 2012; the Particle Analysis by Laser Mass Spectrometry, PALMS, Murphy, 2007), (2) laser induced incandescence (LII) methods (e.g., the High Sensitivity Laser Induced Incandescence instrument, HS-LII, Schulz et al., 2006; the Single Particle Soot Photometer, SP2, Schwarz et al., 2006), and (3) the Soot particle Aerosol Mass Spectrometer (SP-AMS) which is a combination of the aerosol mass spectrometric technique and the LII technique (Onasch et al., 2012).

Despite several inter-comparison studies (e.g., Kondo et al., 2011b; Laborde et al., 2013), consistency of BC mass quantified by different types of measurement principles has not been well addressed. Nevertheless, each kind of technique has its uncertainty and limitations (Baumgardner et al., 2012). As for thermal-optical methods, a major problem is that a substantial fraction of organic species can be transformed into materials whose thermal and optical behaviors are quite similar to EC (these materials are usually termed char OC or pyrolysis OC; Yang and Yu, 2002). Previous studies conducted at urban locations such as Fresno, CA (Chow et al., 2004), Pittsburgh, PA (Subramanian et al., 2006), Milan, Italy (Piazzalunga et al., 2011), and Beijing, China (Cheng et al., 2012) typically suggested that thermal-optical methods tend to underestimate BC mass due to uncertainties introduced by char OC. For example, it was observed that water (Piazzalunga et al., 2011) or organic solvent (Cheng et al., 2012) extraction, which removes a substantial fraction of OC and consequently reduces the char OC formation (Subramanian et al., 2006), could lead to a considerable increase in the measured EC concentration of urban aerosol. However, uncertainties in the thermal-optical determination of BC mass have not been well characterized for primary emissions from combustion sources, limiting our ability to evaluate BC inventories and thus the modeled distribution and climate impacts of BC. This is particularly true for biomass burning which is the largest BC source globally (Bond et al., 2013).

On the other hand, the absorption coefficient is typically quantified by optical instruments, most of which are based on the measurement of the change in light transmittance through a filter due to the deposition of aerosol particles (Moosmüller et al., 2009). Examples of instruments using the filter-based technique include the Aethalometer (Hansen et al., 1984), the Particle Soot Absorption Photometer (PSAP; Bond et al., 1999), the Multi-Angle Absorption Photometer (MAAP; Petzold et al., 2005) and the continuous soot monitoring system (COSMOS; Kondo et al., 2011b). Of these instruments, the Aethalometer and PSAP are most commonly used. The latest version of the Aethalometer (model AE33) measures the absorption coefficient at seven wavelengths (i.e., 370, 470, 520, 590, 660, 880 and 950 nm; Drinovec et al., 2015), while the commercial single-wavelength PSAP has been modified to yield absorption measurements at three visible wavelengths (i.e., 467, 530 and 660 nm; Virkkula et al., 2005). Although having been widely used, most of the filter-based techniques suffer from various artifacts that need to be carefully addressed. The following corrections are likely necessary for correction of measured transmittance change (i.e., attenuation) to light absorption (Moosmüller et al., 2009; Lack et al., 2014): (1) the filter loading correction which compensates for the non-linear response of attenuation to the increase of BC loading (i.e., the shadowing effect), (2) the multiple scattering correction which accounts for the enhanced attenuation caused by the scattering of filter fibers, and (3) the particle scattering correction which corrects the enhanced attenuation due to the scattering of loaded particles. Significant efforts have been made to develop and improve empirical corrections for the filter-based instruments. Representative algorithms include those introduced by Weingartner et al. (2003), Arnott et al. (2005), Schmid et al. (2006), Collaud Coen et al. (2010) for the Aethalometer, and those described by Bond et al. (1999), Virkkula et al. (2005) and Ogren (2010) for the PSAP. More recently, an algorithm compensating for the shadowing effect, which is based on the attenuation measurements by two parallel spots, was incorporated into the latest version of the Aethalometer (Drinovec et al., 2015).

A difficult challenge to the filter-based techniques such as Aethalometer and PSAP is that the empirical parameters in the correction algorithms are highly variable depending on aerosol source, chemical composition, mixing state, etc. (e.g., Collaud Coen et al., 2010). Moreover, determination of these empirical parameters is not easily performed in the field, and therefore general corrections calculated during inter-comparison campaigns (e.g., Arnott et al., 2005) are usually applied to all Aethalometer or PSAP units. This is also the case for the COSMOS, although it could reduce the particle scattering effect by volatilizing a substantial fraction of non-BC components prior to particle collection (this is done by a thermal denuder; Kondo et al., 2011b). In contrast to the other filter-based instruments, the MAAP does not rely on empirical corrections; instead, it uses a radiative transfer model to retrieve the absorption coefficient from simultaneous measurement of light transmitted through and scattered back from a particle-loaded fiber filter (Petzold et al., 2005). The MAAP has been suggested to be the most reliable filter-based instrument for aerosol absorption measurements (Andreae and Gelencsér, 2006). However, a basic assumption used in MAAP, i.e., the particle-loaded filter can be treated as a two-layer system consisting of a particle-loaded filter layer and the particle-free filter matrix, might be invalid under some conditions (e.g., in the presence of liquid-like aerosols which will spread throughout filter fibers).

Artifacts associated with the filter-based measurement of aerosol absorption can be completely overcome by directly measuring light absorption on airborne particles. This technique is being used by the photoacoustic spectrometer (PAS; Arnott et al., 1999; Lack et al., 2006), which has become the “standard” method for aerosol absorption measurements (Lack et al., 2014).

The PAS is typically operated at a single wavelength such as 532 nm (e.g., Arnott et al., 1999, 2003, 2005; Lack et al., 2006), whereas the on-going development of multi-wavelength PAS provides additional information about the wavelength dependence of aerosol absorption (e.g., Lewis et al., 2008; Haisch et al., 2012; Lack et al., 2012; Sharma et al., 2013). Until recently, however, light absorption measurements by the PAS are only available for limited source categories. Moreover, despite several laboratory (e.g., Sheridan et al., 2005; Cappa et al., 2008) and field (e.g., Schmid et al., 2006; Lack et al., 2008) studies conducted, comparisons between the PAS and filter-based instruments are still limited and have most frequently focused on either ambient samples or laboratory-generated soot particles.

This study investigated the MAE of biomass burning BC generated by controlled combustion of six kinds of wildland fuels during the Fire Laboratory at Missoula Experiments (FLAME) study, which was conducted at the United Sates Forest Service's (USFS) Fire Sciences Lab (FSL) in Missoula, Montana. For the determination of MAE, filter-based EC concentrations measured by a thermal-optical method were used as the BC mass, while the light absorption measurements were primarily performed by a PAS. Influences of EC measurement uncertainties on MAE estimations are discussed. Based on results from urban aerosol, it is commonly believed that BC mass tends to be underestimated by thermal-optical methods (Chow et al., 2004; Subramanian et al., 2006; Piazzalunga et al., 2011; Cheng et al., 2012). However, here we demonstrate that this is not necessarily the case for biomass burning source emissions. On the other hand, artifacts associated with the filter-based measurement of light absorption are evaluated. Our results suggest that in biomass burning emissions, liquid-like organics may be present that can strongly bias filter-based absorption measurements. This study is expected to be meaningful for a better understanding of BC, especially regarding its mass determination and absorption measurement.

2. Measurements and data analysis

The FSL combustion facility has been described in detail elsewhere (McMeeking et al., 2009). Briefly, the main combustion chamber is a square room (12.4 × 12.4 m) with a height of 19.6 m. An exhaust stack located at the center of the room begins 2.1 m above the fuel bed and extends through the chamber ceiling. An inverted funnel at the bottom of the exhaust stack narrows from a 3.6 m diameter opening to the 1.6 m stack diameter. A sampling platform surrounds the stack at ~16.5 m height where all measurement equipment was deployed, sampling directly from the exhaust stack. Six types of dry fuels (with moisture content of less than 10% of dry mass) were burned, including ponderosa pine wood (PP wood), ponderosa pine needles (PP needle), white pine needles (WP needle), excelsior (made from aspen poplar trees), Savanna grass (SA grass; from Zambia), and sagebrush. The absorption coefficient (b_{abs}) of the smoke was measured continuously at two wavelengths (i.e., 532 and 1047 nm) by a PAS. Furthermore, a total of 20 particulate matter (PM) samples were collected onto quartz-fiber filters and were used for the subsequent thermal-optical analysis. Different combustion phases (i.e., flaming vs. smoldering) were not sampled separately in this study.

The quartz-fiber filters were analyzed for organic carbon (OC) and elemental carbon (EC) using a DRI Model 2001 carbon analyzer (Atmoslytic Inc., CA, USA). OC and EC concentrations were quantified using the IMPROVE (Interagency Monitoring of Protected Visual Environments) temperature protocol. The transmittance charring correction was used to separate OC and EC because the absorption measurement by the carbon analyzer is based on the transmittance signal (as shown in Equation (1)). EC concentrations were then used as the BC mass for the calculation of the mass absorption efficiency. The filter optical transmittance signal was measured at a wavelength of 632 nm throughout the OC and EC analysis, providing an approach to calculate the absorption coefficient (Ram and Sarin, 2009):

$$b^{*}_{abs}\left(\mathrm{Mm^{-1}}\right) = \ln\left(\frac{I_0}{I}\right) \times \frac{A}{V} \quad (1)$$

where I and I_0 are the intensity of transmittance signal measured at the beginning (i.e., when the loaded filter has not been heated) and end (i.e., when all of the loaded carbon has been combusted off the filter) of thermal-optical analysis, respectively, and A is the filter area with particle loading (mm^2), while V is the volume of air sampled (m^3). The mass absorption efficiency can be calculated as:

$$\mathrm{MAE^{*}}\left(\mathrm{m^2/g}\right) = \ln\left(\frac{I_0}{I}\right) \times \frac{A}{V} \times \frac{1}{\mathrm{EC_m}} = \frac{\mathrm{ATN}}{\mathrm{EC_s}} \times 100 \quad (2)$$

where ATN indicates the optical attenuation that equals $\ln(I_0/I)$, while EC_m ($\mu g/m^3$) and EC_s ($\mu g/cm^2$) are the mass concentration and filter loading of EC, respectively. Note that both the absorption coefficient derived from Equation (1) and the mass absorption efficiency derived from Equation (2) are the raw values uncorrected for the artifacts associated with the filter-based measurement of light absorption, thus are specified as b^{*}_{abs} and MAE^{*}, respectively.

In this study, the PAS was operated continuously (i.e., with a time resolution of 3 and 7 s at 532 and 1047 nm, respectively), whereas EC concentrations were measured for filter samples that represent time-integrated averages. Thus, when using the PAS, the mass absorption efficiency is calculated as:

$$\mathrm{MAE}\left(\mathrm{m^2/g}\right) = \frac{\int_{T_1}^{T_2} b_{abs}\,dt}{\mathrm{EC_m} \times (T_2 - T_1)} = \frac{\text{integrated } b_{abs}}{\text{integrated EC}} \quad (3)$$

where T_1 and T_2 are the start and stop time for quartz-fiber filter sampling, respectively, while integrated b_{abs} and integrated EC indicate $\int_{T_1}^{T_2} b_{abs}\,dt$ and $\mathrm{EC_m} \times (T_2 - T_1)$, respectively. Moreover, the aerosol absorption Ångström exponent (AAE), a parameter describing the wavelength-dependence of light absorption, is derived from the PAS measurement as:

$$\mathrm{AAE} = \frac{\ln(\mathrm{MAE_{532}}/\mathrm{MAE_{1047}})}{\ln(1047/532)} \quad (4)$$

where MAE_{532} and MAE_{1047} are the MAE calculated by Equation (3) at 532 and 1047 nm, respectively.

3. Results and discussion

3.1. MAE retrieved from the PAS

MAE_{532} fell within a relatively narrow range of ~7–~9 m^2/g for the majority of the burning cases in this study, whereas substantially lower values were observed during certain burns (Fig. 1). The variation of MAE_{532} was found to be strongly related to the abundance of organic matter (OM). Here the OM abundance was estimated by the OC to EC ratio, although the EC concentrations may not be an ideal measure of BC mass. As shown in Fig. 2(a), MAE_{532} averaged 7.8 ± 0.1 m^2/g (N = 2; termed type-0 smoke) when OC/EC was below 0.3. For the type-0 smoke cases, formation of char OC and thus the char OC-related uncertainties in EC results were virtually negligible, as demonstrated by the roughly constant filter transmittance signal observed in the inert mode of thermal-optical

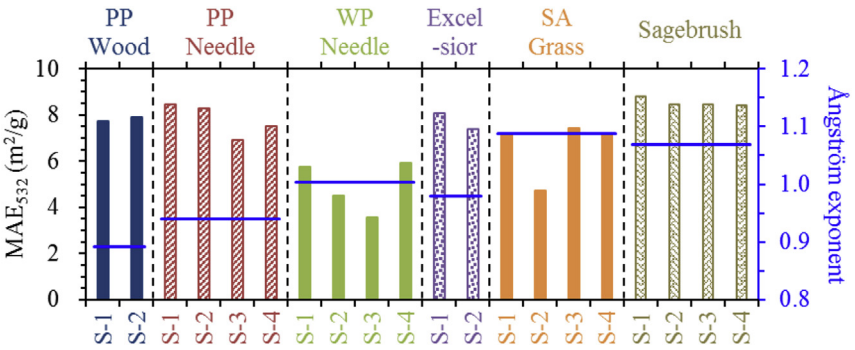

Fig. 1. MAE of biomass burning BC derived from the PAS at a wavelength of 532 nm (bars; left axis). Also shown is the absorption Ångström exponent based on the light absorption measurement by the PAS at 532 and 1047 nm (blue lines; right axis). Two filter samples were collected during the combustion of PP wood and excelsior, whereas four samples were collected for the other biofuels. (For interpretation of the references to colour in this figure legend, the reader is referred to the web version of this article.)

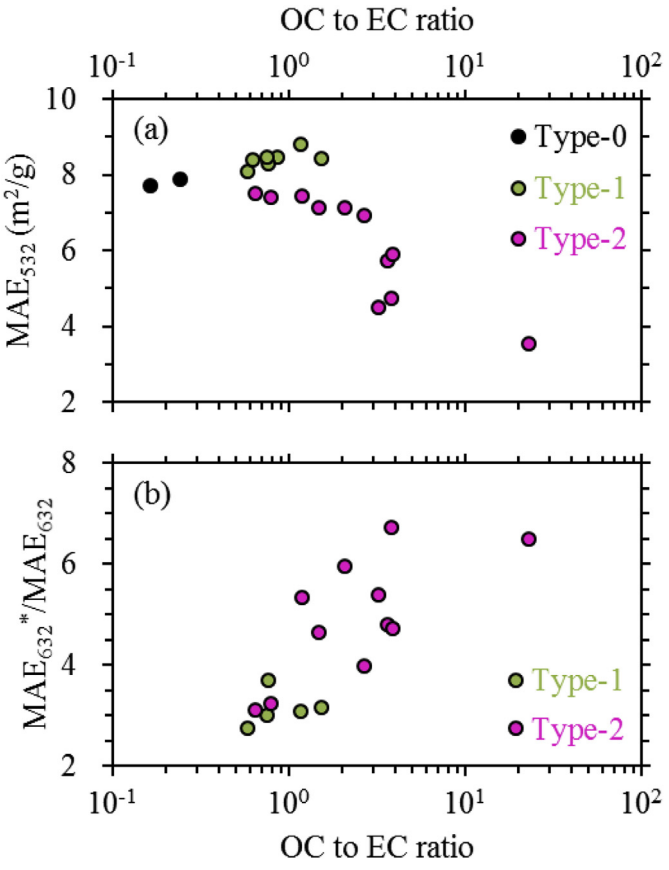

Fig. 2. Relationship between MAE derived from the PAS at a wavelength of 532 nm (i.e., MAE_{532}) and the OC to EC ratio (a). Also shown are the ratios of carbon analyzer to PAS retrieved MAE (i.e., MAE_{632}^{*} to MAE_{632} ratios) versus OC to EC ratios (b). In (b), MAE_{632}^{*} and thus the MAE_{632}^{*} to MAE_{632} ratio are not available for the samples with EC loading above 11 μg C/cm^2 (N = 4; including the two samples collected for the type-0 burning cases, and two of the samples collected for the type-1 burning cases). OC to EC ratio provides an estimation of OM abundance, although EC concentrations may not be an ideal measure of BC mass. We also estimated the OM abundance by the ratio of He carbon to He/O_2 carbon, and observed the same patterns as those shown in Fig. 2 (see Supplementary material). In addition, it was observed that the burning of the same kind of fuel could produce different types of smoke, presumably depending on the combustion condition (see Supplementary material).

analysis (Fig. 3(a)). On the other hand, although BC size distributions were not measured in this study, previous investigations suggested that the mass median diameter (MMD) of BC was about 200 nm in fresh biomass burning emissions (Schwarz et al., 2008; Kondo et al., 2011a; Taylor et al., 2014). Accordingly, an OC to EC mass ratio of 0.3 can be translated to a coating thickness ($T_{coating}$) of ~20 nm, by assuming a concentric core–shell morphology with the BC core diameter (D_{core}) being held fixed at 200 nm, an OM (organic matter) to OC ratio of 1.6 (Aiken et al., 2008) to 2.0 (Turpin and Lim, 2001), a BC density (ρ_{BC}) of 1.8 g/cm^3 (Bond and Bergstrom, 2006), and an OM density (ρ_{OM}) of 1.0–1.4 (Turpin and Lim, 2001; Cappa et al., 2012):

$$T_{coating} = \frac{D_{core}}{2} \times \left[\left(1 + \frac{OC}{EC} \times \frac{OM}{OC} \times \frac{\rho_{BC}}{\rho_{OM}} \right)^{1/3} - 1 \right] \quad (5)$$

According to laboratory experiments (in which graphite particles were coated by organics) and theoretical calculations (using the core–shell model based on Mie theory) by Shiraiwa et al. (2010), organic coating with a thickness of ~20 nm (i.e., a shell to core diameter ratio of ~1.2) will not cause a strong enhancement of light absorption when the BC core diameter is ~200 nm. Moreover, the light absorption enhancement will become even smaller if assuming a non-core-shell morphology (e.g., the BC core is located in an off-center position within the host organic material; Adachi et al., 2010). Thus, amplification of BC light absorption by organic coating should be insignificant at the extremely low OC to EC ratios (i.e., below 0.3) measured in the type-0 smoke cases. This explains why the MAE_{532} measured in the type-0 smoke cases are in good agreement with those suggested for uncoated BC (Bond and Bergstrom, 2006).

As OC/EC became higher, MAE_{532} showed an increasing trend for some of the burning cases (N = 7; referred to as type-1 smoke) with the peak value (8.8 m^2/g, corresponding to a 13% increase relative to 7.8 m^2/g) being observed at an OC/EC of 1.2. The positive correlation between MAE_{532} and OC/EC can readily be attributed to the enhancement of light absorption by BC due to organic coating (Schnaiter et al., 2005; Bond et al., 2006). Using Equation (5) with the same assumptions as mentioned above, an OC to EC ratio of 1.2 corresponds to a coating thickness of ~60 nm. Shiraiwa et al. (2010) suggested that in the case of a core–shell morphology, a coating of ~60 nm can increase the BC light absorption by ~ 50% when the BC core diameter is ~200 nm. However, the observed absorption enhancement (i.e., 13%) was much smaller than the prediction by Shiraiwa et al. (2010), presumably indicating that the mixing state of biomass burning BC cannot be fully described by a simple core–shell morphology.

For the remaining cases (N = 11; termed type-2 smoke), MAE_{532} tended to decrease with the increase of OC/EC and deviated more strongly from 7.8 m^2/g (down to 3.6 m^2/g) once OC/EC exceeded 3.0 (Fig. 2(a)). The negative dependence of MAE_{532} on OC/EC, which is

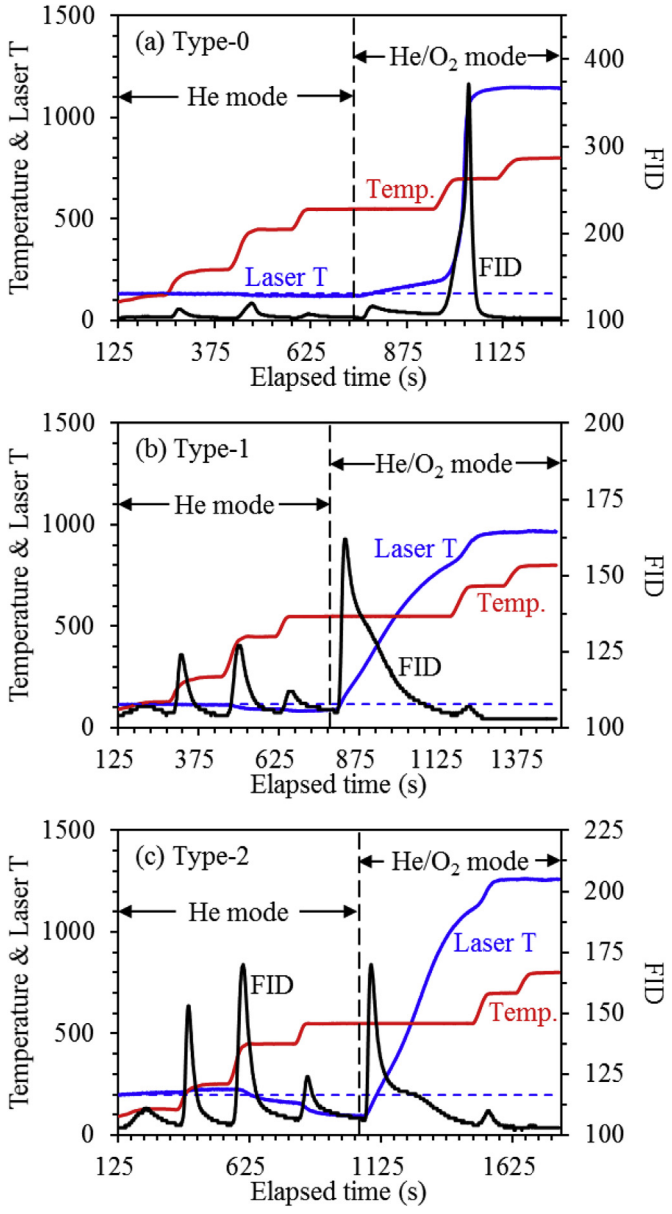

Fig. 3. Example thermograms of samples collected for (a) type-0 smoke (generated by the combustion of PP wood), (b) type-1 smoke (generated by the combustion of sagebrush), and (c) type-2 smoke (generated by the combustion of PP needles). FID, Laser T, and Temp. are the carbon signal measured by the flame ionization detector, the transmittance signal measured at 632 nm, and the temperature, respectively. Drop of filter transmittance during the He mode indicates the formation of char OC. The horizontal dashed lines correspond to the baseline of filter transmittance.

not readily explained by the mixing state of BC, has not been observed in previous studies based on either laboratory experiments or ambient measurements (e.g., Cappa et al., 2012). In addition, several type-2 smoke cases had MAE_{532} values below 5.0 m^2/g, which are too low for BC (Bond et al., 2013; Petzold et al., 2013).

3.2. Evaluation of the relatively low MAE_{532} values observed in the type-2 smoke

Results from the type-2 smoke cases point to the presence of a distinct group of non-BC compounds (e.g., organics) that can reduce the calculated MAE through interfering with the light absorption and/or BC mass measurements. We suggest that the reduction in MAE is most likely caused by an overestimation of BC mass by the thermal-optical method, because mixing of BC with organics will either increase (e.g., when BC and organics are internally mixed or when BC is externally mixed with light-absorbing organics) or have no effect on light absorption (e.g., when BC is externally mixed with non-light-absorbing organics). Moreover, the overestimation of BC mass seems to be more significant for the biomass burning emissions more abundant in OC, as indicated by the negative dependence of MAE_{532} on OC/EC observed in the type-2 smoke cases. For the smoke having the highest OC/EC (23.0), MAE_{532} was as low as 3.6 m^2/g, indicating that the BC mass was overestimated by a factor of at least ~2 (calculated as the ratio of 7.8 m^2/g to 3.6 m^2/g).

As mentioned in the Introduction, uncertainties in the thermal-optical determination of EC mass are strongly associated with char OC. Formation of char OC primarily occurs in the inert mode of thermal-optical analysis, and typically accompanies an apparent drop of filter transmittance and reflectance. Similar to EC, on the other hand, char OC usually requires an oxidizing atmosphere to be combusted off the filter, indicating that carbon evolving in the oxidizing mode of thermal-optical analysis (i.e., He/O_2 carbon) includes both char OC and EC. To classify He/O_2 carbon into char OC and EC, thermal-optical methods use the amount of He/O_2 carbon that is required to increase the filter transmittance (or reflectance) to its initial value as an estimation of char OC. However, char OC will be overestimated (i.e., EC will be biased low) if EC and thus He/O_2 carbon is less light absorbing compared to char OC, whereas char OC will be underestimated (i.e., EC will be biased high) if EC and thus He/O_2 carbon is more light absorbing. Previous studies conducted at urban locations typically suggested that EC is less light absorbing than char OC, resulting in an underestimation of BC mass by thermal-optical methods (Chow et al., 2004; Subramanian et al., 2006; Cheng et al., 2012). Therefore, our finding that BC mass can be significantly overestimated by thermal-optical methods is different from most of the previous studies. Here we suggest several likely explanations for this distinct phenomenon which is observed only in the type-2 burning cases.

(1) In the carbonaceous materials generated by the type-2 burning cases, some distinct organic compounds may be present that can be transformed into char OC having a lower light absorbing capacity compared to EC.
(2) For the majority of the filter samples collected for the type-2 burning cases, the evolution of filter transmittance in the inert mode of thermal-optical analysis exhibited a distinct "increase followed by decrease" pattern (Fig. 3(c)), which was not observed in type-0 or type-1 burning cases. While the decrease phase of filter transmittance can be readily attributed to the formation of char OC, the increase phase is unexpected and seems to indicate the removal (e.g., volatilization) of organic compounds that are light absorbing at the monitoring wavelength of the carbon analyzer (i.e., 632 nm). In this case, decrease of filter transmittance caused by char OC formation will be partially offset by the removal of these light absorbing organics, consequently resulting in an underestimation of char OC (i.e., an overestimation of EC).
(3) The type-2 burning cases can produce light-absorbing OC (i.e., brown carbon) that can be classified as EC. Brown carbon covers a wide range of light absorbing properties, including not only weakly absorbing species such as humic-like substances (the MAE of which is close to zero at 532 nm; Hoffer et al., 2006) but also strongly absorbing particles such as tar balls (the MAE of which was estimated to be slightly lower than that of BC at 550 nm; Alexander et al., 2008). It is not surprising that refractory brown carbon such as tar balls

could be classified as EC during thermal-optical analysis (Hand et al., 2005).

For the type-2 burning cases, we cannot confirm which factor mentioned above is more responsible for the overestimation of BC mass by EC measurements, but it can be concluded that their MAE_{532} values are biased low due to the overestimation of BC mass, and thus should be used with caution.

3.3. MAE retrieved from the carbon analyzer

Fig. 4(a) shows the dependence of ATN measured by the carbon analyzer at a wavelength of 632 nm (ATN_{632}) on filter EC loading (EC_s). ATN_{632} and EC_s correlated strongly ($R^2 = 0.93$; $N = 16$) with a slope of 21.7 ± 0.6 m^2/g, when EC_s was below 11 μg/cm^2. However, the linearity did not extend to EC_s exceeding 11 μg/cm^2 ($N = 4$), indicating that ATN became non-sensitive to the increase of EC_s for these high-loading samples. After excluding the four samples with EC loadings above 11 μg/cm^2, MAE retrieved from the carbon analyzer at 632 nm (MAE_{632}^*) averaged 24.0 ± 4.7 m^2/g.

Before comparing MAE derived from the PAS and the carbon analyzer, the difference in the measurement wavelength needs to be accounted for, which requires the absorption Ångström exponent (AAE). AAE has been shown to vary significantly among different types of biomass smoke and depend strongly on the wavelength range within which the exponent is estimated (e.g., between ~1 and ~3.5 for the wavelength pair of 405 and 870 nm vs. between ~1 and ~2.5 for the wavelength pair of 532 and 870 nm; Lewis et al., 2008). In this study, AAE was calculated based on the light absorption measurement by the PAS at 532 and 1047 nm (Fig. 4(b)), and was found to be between 0.9 and 1.1 (Fig. 1). Using the estimated AAE, MAE_{532} derived from the PAS was then converted to the equivalent value at 632 nm (MAE_{632}):

$$MAE_{632} = MAE_{532} \times \left(\frac{532}{632}\right)^{AAE} \quad (6)$$

MAE_{632} averaged 5.8 ± 1.3 m^2/g for biomass smoke with EC loadings below 11 μg/cm^2. The ratio of MAE_{632}^* to MAE_{632} averaged 4.4 ± 1.3, implying that filter-based, uncorrected measurement of b_{abs} (e.g., by the carbon analyzer) may result in substantial overestimation of MAE values.

The MAE_{632}^* to MAE_{632} ratio did not differ much among the type-1 smoke cases (Fig. 2(b)), with an average of 3.1 ± 0.3 ($N = 5$; two of the type-1 smoke cases had EC loadings above 11 μg/cm^2 and thus were excluded when calculating MAE_{632}^*). Similar to the type-1 smoke, some ambient observations also showed a nearly constant ratio between b_{abs} measured by the PAS and filter-based instruments (the ratio will be termed the overestimation factor hereinafter). For example, compared with the PAS, the Aethalometer overestimated b_{abs} by a factor of ~2.4 and ~3.3 in downtown Toronto (Knox et al., 2009) and at an urban site in Las Vegas, NV (Arnott et al., 2005), respectively, while the overestimation factor was found to be ~1.6 for the PSAP during a study conducted in an agricultural environment in northern Oklahoma (Arnott et al., 2003). In addition, air masses were classified into fresh, semi-aged, and aged categories in the study by Knox et al. (2009), but the air mass history was found to have little influence on the overestimation factor for the Aethalometer. A nearly constant overestimation factor presumably indicates that the filter-based light absorption measurement is mainly biased by the multiple scattering effect due to the filter fibers.

The MAE_{632}^* to MAE_{632} ratio was significantly higher for type-2 smoke (averaging 5.0 ± 1.2; $N = 11$) and showed an apparent OC/EC dependence (Fig. 2(b)). Similar to the type-2 smoke, the overestimation factor for the PSAP was found to increase with the ratio of organic aerosol (OA) to BC mass (OA/BC) during ship-borne measurements performed in the Gulf of Mexico and inland waters near Houston, Texas (Lack et al., 2008). Subramanian et al. (2007) found that liquid-like organics are preferentially emitted during the smoldering combustion phase of biomass burning which is characterized by high emission ratios of OC to EC. Thus, the positive dependence of the MAE_{632}^* to MAE_{632} ratio on OC/EC observed in the type-2 smoke cases might be caused by the redistribution of liquid-like organic compounds around the fiber filters.

4. Conclusions and implications

MAE of biomass burning BC was investigated during the FLAME study. BC mass was quantified by a thermal-optical method, while b_{abs} was primarily measured by a PAS. MAE_{532} values observed at extremely low OC to EC emissions ratios (i.e., below 0.3) were about 7.8 m^2/g, in good agreement with those suggested for uncoated BC. At higher OC to EC ratios, two distinct types of biomass smoke were identified based on the dependence of MAE_{532} on the OC to EC ratio. For the first type, MAE_{532} depended positively on the OC to EC ratio, suggesting the enhancement of BC light absorption by organic coating. For the second type, MAE_{532} depended negatively on the

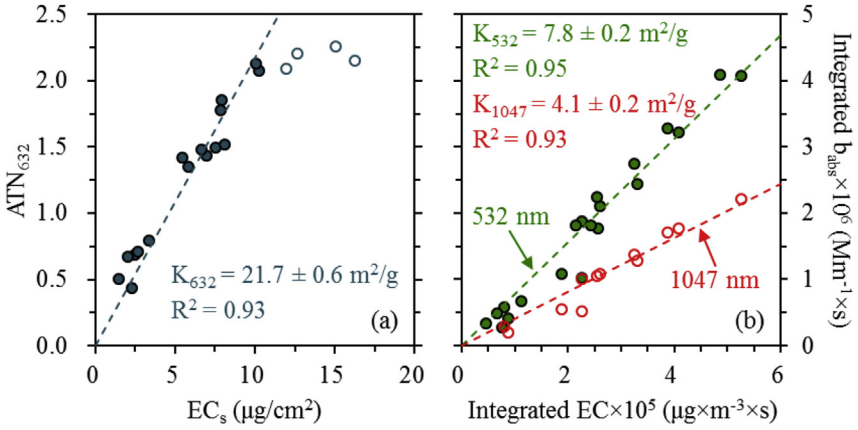

Fig. 4. ATN retrieved from the carbon analyzer as a function of EC loading (a), and the dependence of integrated b_{abs} retrieved from the PAS on integrated EC (b). The dashed lines indicate the linear regression results with K as slope and intercept set as zero. In (a), samples with EC loading above 11 μg C/cm^2 ($N = 4$), which are marked by the open-circles, are not included in the regression since their ATN becomes non-sensitive to the increase of EC loading. These four samples are not used to derive MAE from the carbon analyzer either.

OC to EC ratio; this trend cannot be readily explained by BC mixing state, instead, it indicates an increased overestimation of BC mass by thermal-optical methods at higher OC to EC ratios. In addition, these two types of biomass smoke also differed substantially with respect to artifacts in the filter-based b_{abs}. For the first type, the overestimation of b_{abs} by a filter-based method was less significant and could be estimated by a nearly constant correction factor. In contrast, for the second type, the overestimation of b_{abs} by the filter-based method was much more significant and showed an apparent OC/EC dependence.

Emissions and the resulting distribution and radiative forcing of BC strongly rely on emission factors of BC which are frequently determined by thermal-optical analysis. This study suggests that in some types of biomass burning source emissions (e.g., those having high emission ratios of OC to EC), a distinct group of organic compounds may be present that can result in an overestimation of BC mass by thermal-optical methods. In some cases, BC mass was overestimated by a factor of at least ~2, indicating that present assessments of biomass burning BC emissions might be substantially overestimated. On the other hand, biomass burning emissions may include some liquid-like organics that can complicate filter-based light absorption measurements. Artifacts caused by these liquid-like organics are difficult to account for with correction algorithms, but may be reduced by utilization of a thermal denuder.

Acknowledgment

The first author was supported by the National Natural Science Foundation of China under Grant No. 21307067, by Tsinghua University under Grant No. 20131089241, and by the International Postdoctoral Exchange Fellowship Program. This work was also supported by the Joint Venture Agreement 03-JV-11222049-102 between the USFS, Rocky Mountain Research Station, Research Work Unit Number 4404 and DRI, by the Joint Fire Science Project through NPS Task J8R07060005, by NASA EPSCoR under Cooperative Agreement No. NNX10AR89A, and by NASA ROSES under Grant No. NNX11AB79G.

Appendix A. Supplementary data

Supplementary data related to this article can be found at http://dx.doi.org/10.1016/j.atmosenv.2015.12.045.

References

Adachi, K., Chung, S.H., Buseck, P.R., 2010. Shapes of soot aerosol particles and implications for their effects on climate. J. Geophys. Res. 115, D15206,. http://dx.doi.org/10.1029/2009JD012868.

Aiken, A.C., DeCarlo, P.F., Kroll, J.H., Worsnop, D.R., Huffman, J.A., Docherty, K.S., Ulbrich, I.M., Mohr, C., Kimmel, J.R., Sueper, D., Sun, Y., Zhang, Q., Trimborn, A., Northway, M., Ziemann, P.J., Canagaratna, M.R., Onasch, T.B., Alfarra, M.R., Prevot, A.S.H., Dommen, J., Duplissy, J., Metzger, A., Baltensperger, U., Jimenez, J.L., 2008. O/C and OM/OC ratios of primary, secondary, and ambient organic aerosols with high resolution time-of-flight aerosol mass spectrometry. Environ. Sci. Technol. 42, 4478–4485.

Alexander, D.T.L., Crozier, P.A., Anderson, J.R., 2008. Brown carbon spheres in East Asian outflow and their optical properties. Science 321, 833–836.

Andreae, M.O., Gelencsér, A., 2006. Black carbon or brown carbon? The nature of light-absorbing carbonaceous aerosols. Atmos. Chem. Phys. 6, 3131–3148.

Arnott, W.P., Moosmüller, H., Rogers, C.F., Jin, T.F., Bruch, R., 1999. Photoacoustic spectrometer for measuring light absorption by aerosol: instrument description. Atmos. Environ. 33, 2845–2852.

Arnott, W.P., Moosmüller, H., Sheridan, P.J., Ogren, J.A., Raspet, R., Slaton, W.V., Hand, J.L., Kreidenweis, S.M., Collett Jr., J.L., 2003. Photoacoustic and filter-based ambient aerosol light absorption measurements: instrument comparisons and the role of relative humidity. J. Geophys. Res. 108, 4034,. http://dx.doi.org/10.1029/2002JD002165.

Arnott, W.P., Hamasha, K., Moosmüller, H., Sheridan, P.J., Ogren, J.A., 2005. Towards aerosol light-absorption measurements with a 7-wavelength aethalometer: evaluation with a photoacoustic instrument and 3-wavelength nephelometer. Aerosol Sci. Technol. 39, 17–29.

Baumgardner, D., Popovicheva, O., Allan, J., Bernardoni, V., Cao, J., Cavalli, F., Cozic, J., Diapouli, E., Eleftheriadis, K., Genberg, P.J., Gonzalez, C., Gysel, M., John, A., Kirchstetter, T.W., Kuhlbusch, T.A.J., Laborde, M., Lack, D., Müller, T., Niessner, R., Petzold, A., Piazzalunga, A., Putaud, J.P., Schwarz, J., Sheridan, P., Subramanian, R., Swietlicki, E., Valli, G., Vecchi, R., Viana, M., 2012. Soot reference materials for instrument calibration and intercomparisons: a workshop summary with recommendations. Atmos. Meas. Tech. 5, 1869–1887.

Bond, T.C., Anderson, T.L., Campbell, D., 1999. Calibration and intercomparison of filter-based measurements of visible light absorption by aerosols. Aerosol Sci. Technol. 30, 582–600.

Bond, T.C., Bergstrom, R.W., 2006. Light absorption by carbonaceous particles: an investigative review. Aerosol Sci. Technol. 40, 27–67.

Bond, T.C., Doherty, S.J., Fahey, D.W., Forster, P.M., Berntsen, T., DeAngelo, B.J., Flanner, M.G., Ghan, S., Kärcher, B., Koch, D., Kinne, S., Kondo, Y., Quinn, P.K., Sarofim, M.C., Schultz, M.G., Schulz, M., Venkataraman, C., Zhang, H., Zhang, S., Bellouin, N., Guttikunda, S.K., Hopke, P.K., Jacobson, M.Z., Kaiser, J.W., Klimont, Z., Lohmann, U., Schwarz, J.P., Shindell, D., Storelvmo, T., Warren, S.G., Zender, C.S., 2013. Bounding the role of black carbon in the climate system: a scientific assessment. J. Geophys. Res. 118 http://dx.doi.org/10.1002/jgrd.50171, 5380–5552.

Bond, T.C., Habib, G., Bergstrom, R.W., 2006. Limitations in the enhancement of visible light absorption due to mixing state. J. Geophys. Res. 111, D20211,. http://dx.doi.org/10.1029/2006JD007315.

Buseck, P.R., Adachi, K., Gelencsér, A., Tompa, É., Pósfai, M., 2014. Ns-Soot: a material-based term for strongly light-absorbing carbonaceous particles. Aerosol Sci. Technol. 48, 777–788.

Cappa, C.D., Lack, D.A., Burkholder, J.B., Ravishankara, A.R., 2008. Bias in filter-based aerosol light absorption measurements due to organic aerosol loading: evidence from laboratory measurements. Aerosol Sci. Technol. 42, 1022–1033.

Cappa, C.D., Onasch, T.B., Massoli, P., Worsnop, D.R., Bates, T.S., Cross, E.S., Davidovits, P., Hakala, J., Hayden, K.L., Jobson, B.T., Kolesar, K.R., Lack, D.A., Lerner, B.M., Li, S.M., Mellon, D., Nuaaman, I., Olfert, J.S., Petäjä, T., Quinn, P.K., Song, C., Subramanian, R., Williams, E.J., Zaveri, R.A., 2012. Radiative absorption enhancements due to the mixing state of atmospheric black carbon. Science 337, 1078–1081.

Cavalli, F., Viana, M., Yttri, K.E., Genberg, J., Putaud, J.P., 2010. Toward a standardized thermal-optical protocol for measuring atmospheric organic and elemental carbon: the EUSAAR protocol. Atmos. Meas. Tech. 3, 79–89.

Cheng, Y., Duan, F.K., He, K.B., Du, Z.Y., Zheng, M., Ma, Y.L., 2012. Intercomparison of thermal-optical method with different temperature protocols: Implications from source samples and solvent extraction. Atmos. Environ. 61, 453–462.

Chow, J.C., Watson, J.G., Chen, L.A., Arnott, W.P., Moosmüller, H., 2004. Equivalence of elemental carbon by thermal/optical reflectance and transmittance with different temperature protocols. Environ. Sci. Technol. 38, 4414–4422.

Collaud Coen, M., Weingartner, E., Apituley, A., Ceburnis, D., Fierz-Schmidhauser, R., Flentje, H., Henzing, J.S., Jennings, S.G., Moerman, M., Petzold, A., Schmid, O., Baltensperger, U., 2010. Minimizing light absorption measurement artifacts of the aethalometer: evaluation of five correction algorithms. Atmos. Meas. Tech. 3, 457–474.

Drinovec, L., Močnik, G., Zotter, P., Prévôt, A.S.H., Ruckstuhl, C., Coz, E., Rupakheti, M., Sciare, J., Müller, T., Wiedensohler, A., Hansen, A.D.A., 2015. The "dual-spot" aethalometer: an improved measurement of aerosol black carbon with real-time loading compensation. Atmos. Meas. Tech. 8, 1965–1979.

Haisch, C., Menzenbach, P., Bladt, H., Niessner, R., 2012. A wide spectral range photoacoustic aerosol absorption spectrometer. Anal. Chem. 84, 8941–8945.

Hand, J.L., Malm, W.C., Laskin, A., Day, D., Lee, T., Wang, C., Carrico, C., Carrillo, J., Cowin, J.P., Collett Jr., J., Iedema, M.J., 2005. Optical, physical, and chemical properties of tar balls observed during the Yosemite aerosol characterization Study. J. Geophys. Res. 110, D21210,. http://dx.doi.org/10.1029/2004JD005728.

Hansen, A.D.A., Rosen, H., Novakov, T., 1984. The aethalometer – an instrument for the real-time measurement of optical absorption by aerosol particles. Sci. Total Environ. 36, 191–196.

Hoffer, A., Gelencsér, A., Guyon, P., Kiss, G., Schmid, O., Frank, G.P., Artaxo, P., Andreae, M.O., 2006. Optical properties of humic-like substances (HULIS) in biomass-burning aerosols. Atmos. Chem. Phys. 6, 3563–3570.

Kondo, Y., Matsui, H., Moteki, N., Sahu, L., Takegawa, N., Kajino, M., Zhao, Y., Cubison, M.J., Jimenez, J.L., Vay, S., Diskin, G.S., Anderson, B., Wisthaler, A., Mikoviny, T., Fuelberg, H.E., Blake, D.R., Huey, G., Weinheimer, A.J., Knapp, D.J., Brune, W.H., 2011a. Emissions of black carbon, organic, and inorganic aerosols from biomass burning in North America and Asia in 2008. J. Geophys. Res. 116, D08204. http://dx.doi.org/10.1029/2010JD015152.

Kondo, Y., Sahu, L., Moteki, N., Khan, F., Takegawa, N., Liu, X., Koike, M., Miyakawa, T., 2011b. Consistency and traceability of black carbon measurements made by laser-induced incandescence, thermal-optical transmittance, and filter-based photo-absorption techniques. Aerosol Sci. Technol. 45, 295–312.

Knox, A., Evans, G.J., Brook, J.R., Yao, X., Jeong, C.H., Godri, K.J., Sabaliauskas, K., Slowik, J.G., 2009. Mass absorption cross-section of ambient black carbon aerosol in relation to chemical age. Aerosol Sci. Technol. 43, 522–532.

Laborde, M., Crippa, M., Tritscher, T., Jurányi, Z., Decarlo, P.F., Temime-Roussel, B., Marchand, N., Eckhardt, S., Stohl, A., Baltensperger, U., Prévôt, A.S.H., Weingartner, E., Gysel, M., 2013. Black carbon physical properties and mixing state in the European megacity Paris. Atmos. Chem. Phys. 13, 5831–5856.

Lack, D.A., Cappa, C.D., Covert, D.S., Baynard, T., Massoli, P., Sierau, B., Bates, T.S., Quinn, P.K., Lovejoy, E.R., Ravishankara, A.R., 2008. Bias in filter-based aerosol absorption measurements due to organic aerosol loading: evidence from

ambient measurements. Aerosol Sci. Technol. 42, 1033–1041.
Lack, D.A., Lovejoy, E.R., Baynard, T., Pettersson, A., Ravishankara, A.R., 2006. Aerosol absorption measurement using photoacoustic spectroscopy: Sensitivity, calibration, and uncertainty developments. Aerosol Sci. Technol. 40, 697–708.
Lack, D.A., Moosmüller, H., McMeeking, G.R., Chakrabarty, R.K., Baumgardner, D., 2014. Characterizing elemental, equivalent black, and refractory black carbon aerosol particles: a review of techniques, their limitations and uncertainties. Anal. Bioanal. Chem. 406, 99–122.
Lack, D.A., Richardson, M.S., Law, D., Langridge, J.M., Cappa, C.D., McLaughlin, R.J., Murphy, D.M., 2012. Aircraft instrument for comprehensive characterization of aerosol optical properties, part 2: black and brown carbon absorption and absorption enhancement measured with photo acoustic spectroscopy. Aerosol Sci. Technol. 46, 555–568.
Lewis, K., Arnott, W.P., Moosmüller, H., Wold, C.E., 2008. Strong spectral variation of biomass smoke light absorption and single scattering albedo observed with a novel dual-wavelength photoacoustic instrument. J. Geophys. Res. 113, D16203,. http://dx.doi.org/10.1029/2007JD009699.
McMeeking, G.R., Kreidenweis, S.M., Baker, S., Carrico, C.M., Chow, J.C., Collett Jr., J.L., Hao, W.M., Holden, A.S., Kirchstetter, T.W., Malm, W.C., Moosmüller, H., Sullivan, A.P., Wold, C.E., 2009. Emissions of trace gases and aerosols during the open combustion of biomass in the laboratory. J. Geophys. Res. 114, D19210,. http://dx.doi.org/10.1029/2009JD011836.
Moosmüller, H., Chakrabarty, R.K., Arnott, W.P., 2009. Aerosol light absorption and its measurement: a review. J. Quant. Spectrosc. Radiat. Transfer 110, 844–878.
Murphy, D.M., 2007. The design of single particle laser mass spectrometers. Mass Spectrom. Rev. 26, 150–165.
Onasch, T.B., Trimborn, A., Fortner, E.C., Jayne, J.T., Kok, G.L., Williams, L.R., Davidovits, P., Worsnop, D.R., 2012. Soot particle aerosol mass spectrometer: development, validation, and initial application. Aerosol Sci. Technol. 46, 804–817.
Ogren, J.A., 2010. Comment on "calibration and intercomparison of filter-based measurements of visible light absorption by aerosols". Aerosol Sci. Technol. 44, 589–591.
Petzold, A., Ogren, J.A., Fiebig, M., Laj, P., Li, S.M., Baltensperger, U., Holzer-Popp, T., Kinne, S., Pappalardo, G., Sugimoto, N., Wehrli, C., Wiedensohler, A., Zhang, X.Y., 2013. Recommendations for reporting "black carbon" measurements. Atmos. Chem. Phys. 13, 8365–8379.
Petzold, A., Schloesser, H., Sheridan, P.J., Arnott, W.P., Ogren, J.A., Virkkula, A., 2005. Evaluation of multiangle absorption photometry for measuring aerosol light absorption. Aerosol Sci. Technol. 39, 40–51.
Piazzalunga, A., Bernardoni, V., Fermo, P., Valli, G., Vecchi, R., 2011. Technical note: on the effect of water-soluble compounds removal on EC quantification by TOT analysis in urban aerosol samples. Atmos. Chem. Phys. 11, 10193–10203.
Pratt, K.A., Prather, K.A., 2012. Mass spectrometry of atmospheric aerosols – recent developments and applications. Part II: on-line mass spectrometry techniques. Mass Spectrom. Rev. 31, 17–48.
Ram, K., Sarin, M.M., 2009. Absorption coefficient and site-specific mass absorption efficiency of elemental carbon in aerosols over urban rural and high-altitude sites in India. Environ. Sci. Technol. 43, 8233–8239.
Schmid, O., Artaxo, P., Arnott, W.P., Chand, D., Gatti, L.V., Frank, G.P., Hoffer, A., Schnaiter, M., Andreae, M.O., 2006. Spectral light absorption by ambient aerosols influenced by biomass burning in the Amazon Basin. I: comparison and field calibration of absorption measurement techniques. Atmos. Chem. Phys. 6, 3443–3462.
Schnaiter, M., Linke, C., Möhler, O., Naumann, K.H., Saathoff, H., Wagner, R., Schurath, U., Wehner, B., 2005. Absorption amplification of black carbon internally mixed with secondary organic aerosol. J. Geophys. Res. 110, D19204,. http://dx.doi.org/10.1029/2005JD006046.
Schulz, C., Kock, B.F., Hofmann, M., Michelsen, H., Will, S., Bougie, B., Suntz, R., Smallwood, G., 2006. Laser-induced incandescence: recent trends and current questions. Appl. Phys. B 83, 333–354.
Schwarz, J.P., Gao, R.S., Fahey, D.W., Thomson, D.S., Watts, L.A., Wilson, J.C., Reeves, J.M., Darbeheshti, M., Baumgardner, D.G., Kok, G.L., Chung, S.H., Schulz, M., Hendricks, J., Lauer, A., Kärcher, B., Slowik, J.G., Rosenlof, K.H., Thompson, T.L., Langford, A.O., Loewenstein, M., Aikin, K.C., 2006. Single-particle measurements of midlatitude black carbon and light-scattering aerosols from the boundary layer to the lower stratosphere. J. Geophys. Res. 111, D16207,. http://dx.doi.org/10.1029/2006JD007076.
Schwarz, J.P., Gao, R.S., Spackman, J.R., Watts, L.A., Thomson, D.S., Fahey, D.W., Ryerson, T.B., Peischl, J., Holloway, J.S., Trainer, M., Frost, G.J., Baynard, T., Lack, D.A., de Gouw, J.A., Warneke, C., Del Negro, L.A., 2008. Measurement of the mixing state, mass, and optical size of individual black carbon particles in urban and biomass burning emissions. Geophys. Res. Lett. 35, L13810,. http://dx.doi.org/10.1029/2008GL033968.
Sharma, N., Arnold, I.J., Moosmüller, H., Arnott, W.P., Mazzoleni, C., 2013. Photoacoustic and nephelometric spectroscopy of aerosol optical properties with a supercontinuum light source. Atmos. Meas. Tech. 6, 3501–3513.
Sheridan, P.J., Arnott, W.P., Ogren, J.A., Andrews, E., Atkinson, D.B., Covert, D.S., Moosmüller, H., Petzold, A., Schmid, B., Strawa, A.W., Varma, R., Virkkula, A., 2005. The Reno Aerosol Optics Study: an evaluation of aerosol absorption measurement methods. Aerosol Sci. Technol. 39, 1–16.
Shiraiwa, M., Kondo, Y., Iwamoto, T., Kita, K., 2010. Amplification of light absorption of black carbon by organic coating. Aerosol Sci. Technol. 44, 46–54.
Subramanian, R., Khlystov, A.Y., Robinson, A.L., 2006. Effect of peak inert-mode temperature on elemental carbon measured using thermal-optical analysis. Aerosol Sci. Technol. 40, 763–780.
Subramanian, R., Roden, C.A., Boparai, P., Bond, T.C., 2007. Yellow beads and missing particles: trouble ahead for filter-based absorption measurements. Aerosol Sci. Technol. 41, 630–637.
Taylor, J.W., Allan, J.D., Allen, G., Coe, H., Williams, P.I., Flynn, M.J., Le Breton, M., Muller, J.B.A., Percival, C.J., Oram, D., Forster, G., Lee, J.D., Rickard, A.R., Parrington, M., Palmer, P.I., 2014. Size-dependent wet removal of black carbon in Canadian biomass burning plumes. Atmos. Chem. Phys. 14, 13755–13771.
Turpin, B.J., Lim, H.J., 2001. Species contributions to $PM_{2.5}$ mass concentrations: revisiting common assumptions for estimating organic mass. Aerosol Sci. Technol. 35, 602–610.
Virkkula, A., Ahlquist, N.C., Covert, D.S., Arnott, W.P., Sheridan, P.J., Quinn, P.K., Coffman, D.J., 2005. Modification, calibration and a field test of an instrument for measuring light absorption by particles. Aerosol Sci. Technol. 39, 68–83.
Weingartner, E., Saathoff, H., Schnaiter, M., Streit, N., Bitnar, B., Baltensperger, U., 2003. Absorption of light by soot particles: determination of the absorption coefficient by means of Aethalometers. J. Aerosol Sci. 34, 1445–1463.
Yang, H., Yu, J.Z., 2002. Uncertainties in charring correction in the analysis of elemental and organic carbon in atmospheric particles by thermal/optical methods. Environ. Sci. Technol. 36, 5199–5204.